A cGMP-signaling pathway in a subset of olfactory sensory neurons

Mike R. Meyer*†, Albert Angele*†, Elisabeth Kremmer‡, U. Benjamin Kaupp†, and Frank Müller†§

†Institut für Biologische Informationsverarbeitung, Forschungszentrum Jülich, D-52425 Jülich, Germany; and ‡Institut für Molekulare Immunologie, GSF-Forschungszentrum für Umwelt und Gesundheit, Marchioninistrasse 25, D-81377 München, Germany

Edited by David L. Garbers, University of Texas Southwestern Medical Center, Dallas, TX, and approved July 10, 2000 (received for review March 27, 2000)

It is well established that signal transduction in sensory neurons of the rat olfactory epithelium involves a cAMP-signaling pathway. However, a small number of olfactory neurons specifically express cGMP-signaling components, namely a guanylyl cyclase (GC-D) and a cGMP-stimulated phosphodiesterase (PDE2). Here, we show that this subset of olfactory neurons expressing GC-D and PDE2 does also express the subunit of a cGMP-selective cyclic nucleotide-gated (CNG) channel that has been previously identified in cone photoreceptors. Further, components of the prototypical cAMP-signaling pathway could not be detected in this subpopulation of cells. These results imply that these neurons use an alternative signaling pathway, with cGMP as the intracellular messenger, and that, in these cells, the receptor current is initiated by the opening of cGMP-gated channels.

The binding of odorants to receptors in the ciliary membrane of olfactory sensory neurons (OSNs) initiates the odorant signal. A cAMP-signaling pathway is thought to be involved in mammalian chemosensory transduction in most, if not all, OSNs (Fig. 1; for review see ref. 1). This pathway consists of serpentine odorant receptors (ref. 2; for review see ref. 3), coupled to type III adenylyl cyclase (ACIII) (4) through a G protein (G_{olf}) (4, 5). The ensuing rise in cAMP concentration (6) opens cyclic nucleotide-gated (CNG) channels and initiates a depolarizing response of the OSN (7). The CNG channel is exquisitely sensitive to cAMP; however, it does not discriminate well between cAMP and cGMP [$K_{1/2}$ (constant of half-maximal activation) values of activation of 3.0 and 1.6 μM, respectively] (7, 8). The ligand sensitivity and selectivity is accomplished by the assembly of three different channel subunits, α3, α4, and β1b (9, 10). In contrast, the CNG channels from rod and cone photoreceptors both have evolved very different cAMP vs. cGMP sensitivities, resulting in channels that are highly cGMP selective (11, 12).

A small population of olfactory neurons that project to a group of atypical glomeruli in the olfactory bulb, named necklace glomeruli, expresses an olfactory-specific guanylyl cyclase (GC-D) and a cGMP-stimulated subtype of phosphodiesterase (PDE2) (13, 14). GC-D is a member of the family of receptor-type guanylyl cyclases that become activated by binding of peptide hormones to the extracellular domain (15). Although no ligand has yet been identified for GC-D, this group of OSNs may not respond to normal odorants but to ligands that control some aspects of reproductive behavior (14, 16, 17).

For a cGMP-signaling pathway in this subset of OSNs, three different scenarios can be envisioned. These neurons could also engage a cAMP-signaling pathway involving the same or similar signaling components as other olfactory neurons. Within this framework, the chief function of cGMP could be in negative feedback, by stimulating the breakdown of cAMP via the cGMP-regulated PDE2 (Fig. 1). A conceptual problem this model suffers from is that the CNG channels' ligand selectivity is poor and a rise in cGMP itself might activate the CNG channel before cGMP becomes degraded by PDE2. Alternatively, cAMP-signaling components could be lacking altogether, with cGMP serving as the principal intracellular messenger that mediates the response of this population of OSNs (Fig. 1). Finally, these neurons could host both G protein-coupled chemoreceptors and receptor guanylyl cyclases that feed into independent cAMP- and cGMP-signaling pathways.

We set out to test the hypothesis that a cGMP-selective CNG channel represents the final target of a cGMP-signaling pathway in these OSNs. We have identified a cGMP-selective isoform of a CNG channel α-subunit that had previously been characterized in cone photoreceptors (α2) and that is strictly colocalized with GC-D and PDE2 in the olfactory epithelium. Most significantly, all components of the canonical cAMP-signaling pathway are absent from this subset of OSNs. Our results demonstrate that cGMP is the messenger in a subset of OSNs and that it is anticipated that a receptor current is produced by a cGMP-selective CNG channel after activation of GC-D by unknown ligand(s).

Methods

Cloning of α2 cDNA. Cloning of cDNA encoding a CNG channel α2 subunit from rat olfactory epithelium was accomplished in several steps. First, we performed nested PCR on olfactory first strand cDNA by using specific primers derived from the rat "CNGgust" channel sequence (18). Overlapping fragments were amplified, spanning the region from I79 to D670 of the deduced amino acid sequence. Identical fragments were amplified by using retinal cDNA as template. Initially we failed to clone the missing 5′ end of the channel cDNA from olfactory epithelium by the 5′RACE (rapid amplification of cDNA ends)-PCR technique, but were successful using retinal cDNA. We then verified by PCR by using specific primers derived from the 5′ end of the retinal cDNA that this sequence also exists in cDNA from the olfactory epithelium. For the amplification of 3′ regions, one round of PCR (40 cycles) was sufficient. For the amplification of the 5′ region, nested PCR (2×30 or 2×40 cycles) was used. PCR experiments indicate that the α2 message was more abundant in the retina than in the olfactory epithelium. We obtained two 5′-fragments from rat olfactory epithelium. The sequence of the shorter fragment was identical with the 5′-end of the retinal α2a sequence. The longer fragment contained an insertion of 114 bp (deduced amino acid sequence: S36–R73). The final

This paper was submitted directly (Track II) to the PNAS office.

Abbreviations: CNG channels, cyclic nucleotide-gated channels; PDE, phosphodiesterase; GC, guanylyl cyclase; AC, adenylyl cyclase; OSN, olfactory sensory neuron; CaM, calmodulin; $K_{1/2}$, constant of half-maximal activation; MBP, maltose-binding protein.

Data deposition: The sequences reported in this paper have been deposited in the GenBank database (accession nos. AJ272428 and AJ272429).

*M.R.M. and A.A. contributed equally to this work.

§To whom reprint requests should be addressed at: Forschungszentrum Jülich, Institut für Biologische Informationsverarbeitung-1, 52425 Jülich, Germany. E-mail: f.mueller@fz-juelich.de.

The publication costs of this article were defrayed in part by page charge payment. This article must therefore be hereby marked "*advertisement*" in accordance with 18 U.S.C. §1734 solely to indicate this fact.

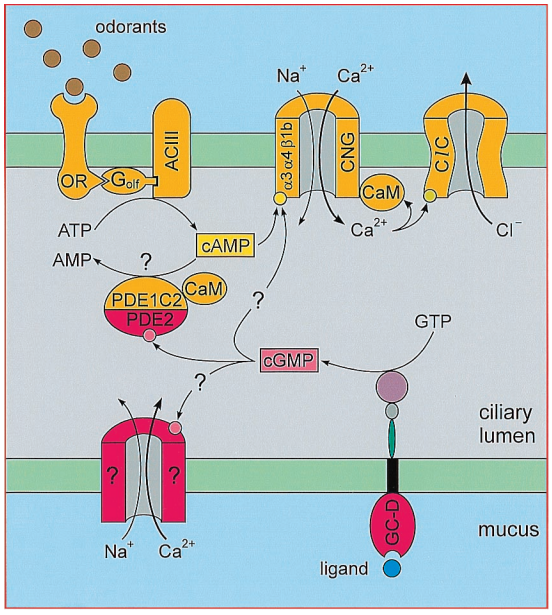

Fig. 1. Two alternative hypotheses of cGMP signaling in a subset of OSNs. (*Upper*) An odorant receptor (OR) activates a cAMP-signaling pathway involving a G protein (G_{olf}), an adenylyl cyclase (ACIII), a cyclic nucleotide-gated (CNG) channel ($\alpha3\alpha4\beta1b$), and a chloride channel (ClC). The cAMP is degraded by a CaM-dependent phosphodiesterase (PDE1C2). (*Lower*) Components of a cGMP-signaling pathway and putative targets of cGMP: receptor guanylyl cyclase GC-D; cGMP-regulated PDE2; an unknown cGMP-regulated ion channel; and the known CNG channel of the cAMP-signaling pathway.

clones, $\alpha2a$ and $\alpha2b$, were constructed from overlapping PCR fragments.

Antibodies Against $\alpha2$ and $\alpha3$ Channel Subunits. Rabbit polyclonal antibody FPc66K was obtained after immunization with a maltose-binding protein (MBP)-fusion protein of the C-terminal region of the $\alpha2$ subunit (amino acids K581–D670). The antibody was purified by sequential affinity chromatography using columns with either immobilized MBP or MBP-fusion proteins. The same fusion protein was used to produce monoclonal antibody CNC9C1. Monoclonal antibody CRO3B10 was raised against an MBP-fusion protein of the C-terminal region of rat $\alpha3$ (amino acids Y482–E664). Immunization of C57BL/6 mice and fusion of immune spleen cells were performed according to standard procedures.

Electrophysiological Recordings. Rat $\alpha2a$ and $\alpha2b$ were subcloned into pcDNAI Amp vector (Invitrogen). A Kozak sequence was introduced before the initiating ATG codon. HEK293 cells were transiently transfected (19). Ligand sensitivity was determined in excised inside-out membrane patches. The bath and pipet solutions contained 100 mM KCl/10 mM EGTA/10 mM Hepes (pH 7.4)/KOH. For CaM experiments, patches were first superfused (1 min) with EGTA-containing solution to remove endogenous CaM that might have adhered to the channel protein. Subsequently, patches were exposed to a solution containing 50 μM free Ca^{2+} (0.8 mM $CaCl_2$ and 2 mM nitrilotriacetic acid) and cGMP and CaM as indicated.

Immunohistochemistry. Retinae and olfactory epithelia of 3-wk-old Sprague–Dawley rats were prepared by immersion fixation in 4% paraformaldehyde in phosphate buffer for 40 min, followed by cryoprotection. After freezing, coronal sections were cut in a cryostat, stained according to standard immunocytochemistry protocols (10) and were examined by using a confocal laser scanning microscope (Leica TCS). In double-labeling experiments, intensities of excitation light and filter settings were carefully adjusted to completely suppress crosstalk between the fluorescence detection channels.

Primary antibodies were as follows: anti-PDE2 (chicken), 1:100; FPc66K against rat $\alpha2$ (rabbit), 1:4,000; CNC9C1 against $\alpha2$ (mouse), 1:50; I-055 against GC-D (rabbit), 1:3,000; anti-ACIII (rabbit), 1:1,500; FPc21K against rat $\beta1$ (rabbit), 1:1,600; anti-G_{olf}/G_s (rabbit), 1:1,600; and CRO3B10 against rat $\alpha3$ (mouse), 1:300. Secondary antibodies (raised in donkey) were as follows: anti-chicken DTAF, 1:50; anti-rabbit Cy3, 1:1,000; and anti-mouse Cy5, 1:100. In some experiments, FPc66K was visualized with a biotinylated secondary antibody (1:1,000) and extravidin-horseradish peroxidase (HRP) (1:300), using diaminobenzidine as chromogen (10). The anti-PDE2 antibody was a gift of J. Beavo, GC-D antiserum I-055 was a gift of D. Garbers, FPc21K and anti-G_{olf}/G_s were gifts of H. G. Körschen and I. Boekhoff, respectively. Anti-ACIII was from Santa Cruz Biotechnology, fluorescence-labeled secondary antibodies from Dianova (Hamburg, Germany), and biotinylated antibodies and extravidin-HRP from Sigma.

Results

Cloning of $\alpha2$ Subunit from OSNs. The CNG channel in chemosensory cilia is composed of three different subunits, designated $\alpha3$, $\alpha4$, and $\beta1b$ (9, 10). We analyzed by PCR the expression in rat olfactory epithelium of additional CNG channel subunits. In particular, we searched for the $\alpha2$ subunit, which forms highly cGMP-selective CNG channels. This subunit was first identified in cone photoreceptors (20–23), but alternative splicing of the $\alpha2$ gene gives rise to channels that differ in their N-terminal regions in several tissues, including testis, kidney, heart, pineal, and taste buds (18, 20, 21, 23–25). The nucleotide sequence of the rat $\alpha2$ subunit expressed in taste buds [referred to as CNGgust (18)] was used to design primers for PCR. As template, first strand cDNA synthesized from rat olfactory poly(A^+) RNA was used. Two $\alpha2$ cDNAs that originate from alternative splicing were constructed from PCR products (see below and *Methods*). Assigning the initiating methionine to the first ATG codon in frame with a stop codon, the shorter form ($\alpha2a$, 1,975 nucleotides) is predicted to encode a 632-aa protein; the longer form ($\alpha2b$, 2,089 nucleotides) a 670-aa protein (Fig. 2).

The nucleotide sequences of CNGgust and $\alpha2a/b$ are identical downstream of nucleotide 219 (aa V74 to D670 of $\alpha2b$), yet bear no sequence similarity (amino acids M1 to R73) upstream of the V74 codon. Moreover, the N-terminal region of CNGgust is significantly shorter than that of other $\alpha2$ orthologs, whereas the longer N-terminal regions of $\alpha2a/b$ and all known $\alpha2$ orthologs are highly conserved. Because R73/V74 demarcate an exon-exon boundary, we suggest that CNGgust represents a partial clone of rat $\alpha2$ whose 5′ region could carry intronic sequences.

To compare which of the $\alpha2a$ and $\alpha2b$ splice forms are expressed in rat retina and olfactory epithelium, cDNA encoding the N-terminal region up to transmembrane segment S2 was amplified by a set of specific primers. Amplification of olfactory cDNA produced fragments of 483 bp and 597 bp, whereas only the 483-bp fragment was amplified from retinal cDNA. The larger 597-bp fragment contains a 114-bp insertion that corresponds to exon 3 of $\alpha2$ orthologs (Fig. 2; amino acid sequence highlighted by gray background). Whereas the functional significance of the $\alpha2$ splice variants is not known, alternative usage of exon 3 would change a CaM-binding motif (Fig. 2*B*) (25, 26) that is encoded by the 5′ end of exon 4 and the 3′ region of the preceding exon (see below).

The $\alpha2$ Subunit Is Expressed in a Subset of OSNs. The expression pattern of the $\alpha2$ subunit in the olfactory epithelium was examined with the affinity-purified antiserum FPc66K (anti-$\alpha2$).

Fig. 2. Primary structure of the rat α2b channel. (*A*) The exon, which is missing in the cDNA of α2a, is highlighted by gray background. The transmembrane segments S1–S6, the pore region, and the cyclic-nucleotide (cNMP)-binding domain are indicated. Established intron positions (18) are indicated (filled triangles). Open triangles indicate intron positions that were not determined by genomic sequencing, but could be deduced because of the intron-exon-structure of α2 orthologs (23, 25) and the existence of consensus sites for exon-exon boundaries. (*B*) Comparison of the putative CaM-binding sites of α2a and α2b. Because of alternative usage of exon 3, rat α2a and α2b possess different putative CaM-binding sites. The position of the amino acids is indicated on the right (for α2b). The 1–5-8–14 motif (26, 51) of the putative CaM-binding sites is indicated (numbers at the top).

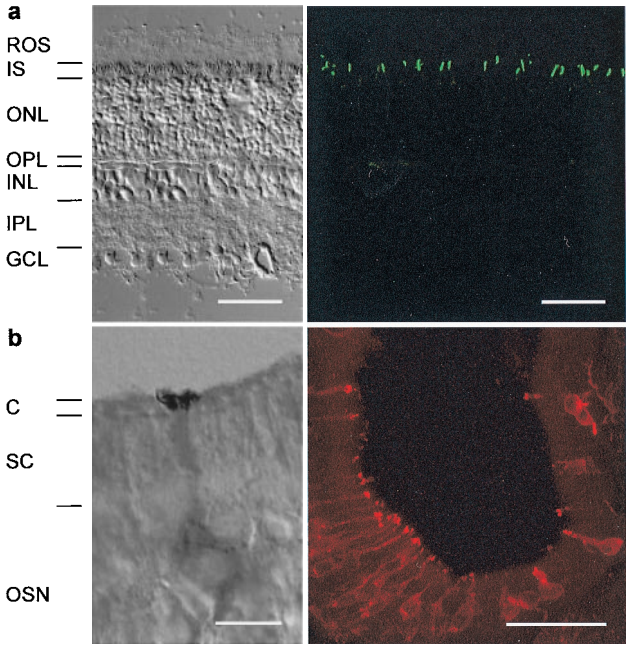

Fig. 3. Immunohistochemical localization of the α2 subunit. (*a*) Section through the rat retina. (*Left*) Differential interference contrast; (*Right*) anti-α2 immunofluorescence in cone outer segments. ROS, rod outer segments; IS, inner segments; ONL, outer nuclear layer; OPL, outer plexiform layer; INL, inner nuclear layer; IPL, inner plexiform layer; GCL, ganglion cell layer. (*b*) Coronal sections through the rat olfactory epithelium. (*Left*) Anti-α2 immunoreactivity shown by dark diaminobenzidine reaction product. Cilia of a single cell are strongly stained; weaker staining is found throughout the cell body. (*Right*) Labeled cells are preferentially found in recesses of the olfactory turbinates close to the cribriform plate. C, ciliary layer; SC, supporting cell layer; OSN, somata of olfactory sensory neurons. Scale bars = 50 μm in *a* and *b Right*; and 10 μm in *b Left*.

The antiserum is directed against the C terminus of the rat α2 and will not discriminate between N-terminal splice variants. We tested the anti-α2 serum by immunocytochemistry on vertical sections of the rat retina (Fig. 3*a*). On the left, the retinal layers are shown by differential interference contrast (DIC) optics. On the right, strong anti-α2 immunofluorescence is observed in cone outer segments, which are readily identified by their typical morphology and their location at the inner segment (IS)/rod outer segment (ROS) border. The anti-α2 serum was used under identical conditions to localize α2 in rat olfactory epithelium. We detected immunolabeling in a sparse population of OSNs (Fig. 3*b*). Typically, the cilia of the neurons were strongly labeled, whereas dendrite and soma showed much weaker labeling, often in a punctate fashion (Fig. 3*b Left*). In some experiments, only the cilia were stained. Labeled cells were distributed throughout the olfactory epithelium either as single isolated neurons or in small clusters. Often, only a few cells were labeled in a coronal section of the nasal cavity. Larger groups of α2-immunoreactive cells were identified in the recesses of the olfactory turbinates near the cribriform plate (Fig. 3*b Right*).

The α2 Subunit Is Coexpressed with GC-D and PDE2. The distribution of α2 is much like the regional pattern of cells that are labeled with antibodies against PDE2 and GC-D in the mouse olfactory epithelium (14). Using double-labeling immunocytochemistry, we tested whether α2 and PDE2 and GC-D reside in one and the same population of OSNs. Fig. 4*a* shows the immunofluorescent detection of PDE2 in rat olfactory epithelium (*Left*). The cilia of two cells are labeled. In the cell on the right, most cilia can be identified, whereas in the left cell, only few cilia become visible, probably, because the plane of section divided the ciliary bundle. Somata or dendrites were not labeled above background. The middle panel shows the same section with the anti-α2 serum. In this case, also, the soma is faintly labeled in a punctate manner. The right panel shows the merged image of the two fluorescent signals with colocalization of the red and green signals producing a yellow signal. Without exception, PDE2-positive cells were also recognized by the anti-α2 serum (roughly 50 cells).

In the rat, as in mouse olfactory epithelium (14), we found PDE2 and GC-D being coexpressed in the same set of OSNs. Strong PDE2 labeling is observed in the dendritic knob and cilia; weaker immunofluorescence is found throughout the cell (Fig. 4*b Left*). GC-D labeling was usually found in all parts of the cell (*Middle*). In the vast majority of cells tested for double labeling, PDE2 and GC-D were coexpressed. Only a few cells could be counted as just PDE2 or GC-D positive, exhibiting no fluorescence for the other protein. We suspect that these exceptions reflect variabilities in the labeling intensity or level of expression rather than evidence for another subpopulation of cells, lacking either one of the two marker proteins. We confirmed the coexpression of α2 with PDE2 and GC-D by using an independent monoclonal antibody CNC9C1 against α2. Fig. 4*c* shows GC-D immunofluorescence in two cells (*Left*), the detection of α2 with the antibody CNC9C1 (*Middle*), and the merged images (*Right*). A third monoclonal antibody 7D8 stained the same ciliary structures (data not shown). In summary, all three proteins are present in one and the same cell population. We refer to these cells as PDE2/GC-D/α2 cells.

The PDE2/GC-D/α2-Positive Cells Do Not Express Components of the cAMP-Signaling Pathway. Fig. 5*a* illustrates that the PDE2/GC-D/α2-positive cells do not express G_{olf}. Cilia, emanating from the dendritic knobs of three cells, are PDE2 positive (*Left*). An

NEUROBIOLOGY

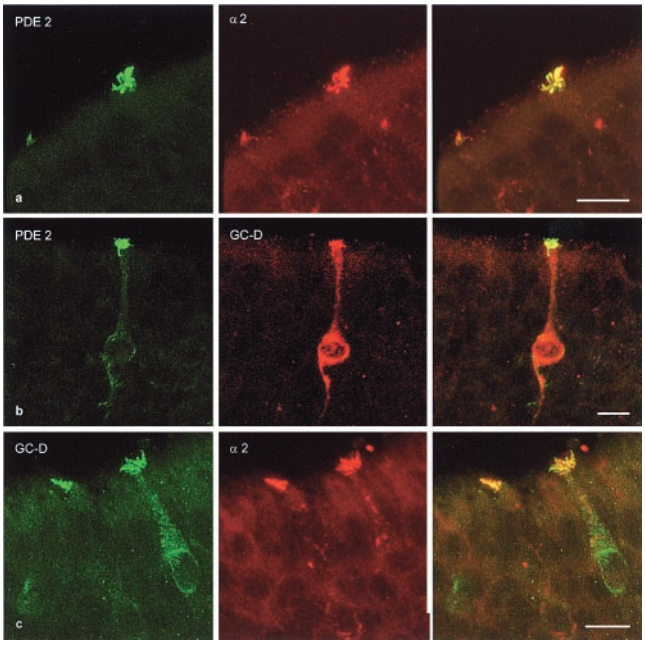

Fig. 4. The α2 subunit is coexpressed with PDE2 and GC-D. (*a Left*) Immunofluorescent detection of PDE2 in cilia of two cells; (*Middle*) anti-α2 immunofluorescence (antibody FPc66K); (*Right*) merged image showing colocalization of PDE2 and α2. (*b Left*) anti-PDE2 immunofluorescence; (*Middle*) anti-GC-D immunofluorescence; (*Right*) merged image; both proteins are colocalized. (*c Left*) anti-GC-D immunofluorescence; (*Middle*) anti-α2 immunofluorescence (antibody CNC9C1); (*Right*) merged image; both proteins are colocalized. Scale bars = 10 μm.

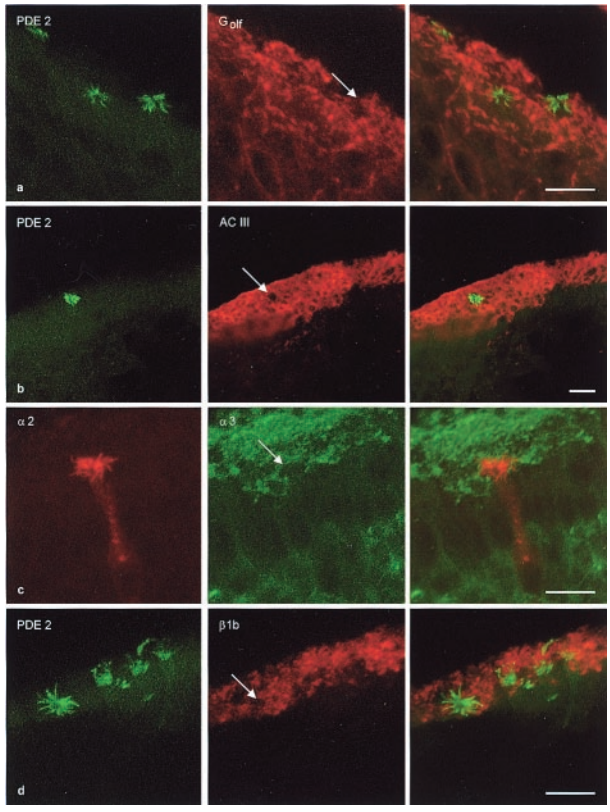

Fig. 5. Components of the olfactory cAMP-signaling pathway are absent from α2-positive neurons. (*a Left*) Cilia of three PDE2-positive cells; plane of section is slightly oblique. (*Middle*) G_{olf}/G_s-positive cilia form a continuous layer; arrow indicates the position of one PDE2-positive ciliary bundle in the red "lawn." (*Right*) Merged image, no colocalization is observed. (*b Left*) Cilia of a PDE2-positive cell; (*Middle*) ACIII-positive cilia form a continuous layer with a hole (arrow); (*Right*) merged image; no colocalization. (*c Left*) Anti-α2 immunofluorescence. (*Middle*) α3-positive cilia; note the hole (arrow). (*Right*) Merged image, no colocalization. (*d Left*) PDE2-positive cilia. (*Middle*) β1 is found throughout the ciliary layer; arrow indicates the position of a PDE2-positive ciliary bundle. (*Right*) Merged image, no colocalization. Scale bars = 10 μm.

antiserum recognizing G_{olf}/G_s stains the ciliary layer homogeneously (*Middle*). The ciliary layer was cut slightly oblique and, therefore, appears rather broad. In the merged image, the PDE2-positive cilia perfectly fill holes present in the red "lawn" of the G_{olf}/G_s-signal; i.e., red and green signals are completely separated and no colocalization can be observed. The same holds for PDE2 and ACIII (Fig. 5*b*), confirming the finding by Juilfs *et al.* (14).

CNG channels in the vast majority of OSNs are composed of α3, α4, and β1b subunits (10). We tested whether α2 is coexpressed with these other channel subunits. Fig. 5*c* shows a double-labeling experiment using anti-α2 serum and the monoclonal antibody CRO3B10 directed against α3. A single, α2-positive cell is observed (*Left*), whereas the ciliary layer is uniformly labeled with the anti-α3 antibody (*Middle*). The layer of supporting cells below the cilia is devoid of fluorescence. Most somata of the OSNs show weak immunofluorescence. The α2-positive cilia fit precisely into a hole at the edge of the ciliary layer (arrow); no colocalization is observed (*Right*). Moreover, the soma of the α2-positive cell lacks α3-immunoreactivity. Finally, in a double-labeling experiment with the antiserum FPc21K, which detects all known β1 splice variants in the retina and olfactory epithelium (10), PDE2 and β1b expression do not overlap (Fig. 5*d*). In our hands, the only available monoclonal antibody 7B11 against the α4 subunit is not useful for immunocytochemistry (10), and, therefore, we cannot say whether the α4 subunit is expressed in the PDE2/GC-D/α2-positive cells. In summary, of the four signaling components we tested, known to be involved in the cAMP-signaling pathway of most OSNs (G_{olf}/G_s, ACIII, α3, and β1b), none could be detected in the PDE2/GC-D/α2-positive cells.

α2 Forms a cGMP-Selective Channel. Channels formed from either the α2a or α2b subunit were characterized electrophysiologically by heterologous expression in HEK 293 cells. Fig. 6*a* shows a family of current-voltage (I/V_m) relations recorded in the inside-out patch configuration at different cGMP concentrations.

The dose-response relations for the α2a and α2b channels at +60 mV are shown in Fig. 6*b*. All currents were normalized to currents recorded at saturating cGMP concentrations. At +60 mV, the currents activated by saturating cAMP and cGMP are identical (Fig. 6*b*), whereas at −60 mV, $I_{max,cAMP}/I_{max,cGMP}$ is roughly 0.7 (data not shown). Solid lines represent fits of the Hill equation $I/I_{max} = c^n/(c^n + K_{1/2}{}^n)$ to the data from α2a channels, and dashed lines from α2b channels. Mean values for the concentration of half-maximal activation $K_{1/2}$ and the Hill coefficient n are summarized in Table 1. The cAMP concentrations needed to activate both channel forms were roughly two orders of magnitude larger than for cGMP, i.e., both channel forms are highly cGMP selective. A high cGMP selectivity is preserved after coexpression of modulatory subunits (β1b or α4, respectively; data not shown). Recently, a second β subunit has been identified that was suggested to be expressed in cone photoreceptors. Coexpression with its cognate α2 subunit produces heteromeric channels that are highly cGMP selective (27). Thus, coexpression of the α2 subunit with all known modulatory subunits gives rise to cGMP-selective channels.

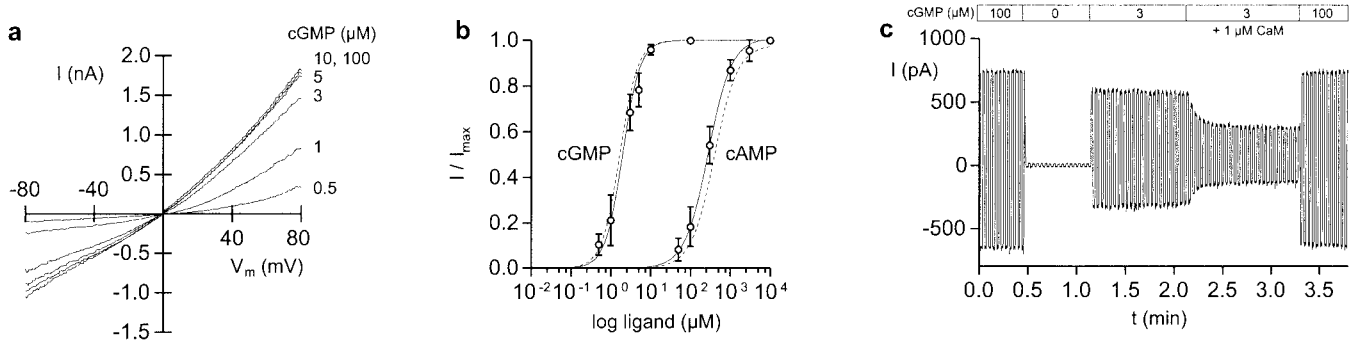

Fig. 6. Properties of heterologously expressed α2 channels. (*a*) Current-voltage (I/V_m) relations of α2a channels in the presence of different cGMP concentrations. (*b*) Dose-response curves for α2a (solid lines) and α2b (dashed lines) at $V_m = +60$ mV. All currents were normalized to currents at saturating cGMP. For clarity, data points and error bars were omitted from dashed traces. (*c*) α2 channels are modulated by CaM. V_m was switched from -40 mV to $+40$ mV in 1-s intervals. The inside-out patch (α2b) was superfused with 100 μM cGMP to record saturating currents, followed by superfusion in 0 μM cGMP. During superfusion with 3 μM cGMP for 1 min, the current stayed constant. With 3 μM cGMP and 1 μM CaM, the current decreased by roughly 50% within 30 s. The current at saturating cGMP (100 μM) was not altered by CaM.

α2 Channels Are Modulated by CaM. The N-terminal region of the α2 subunit carries a putative CaM-binding site similar to that identified in the α3 subunit (25, 28). We assayed whether the channels composed of either splice variant are modulated by binding of CaM. Fig. 6*c* shows an experiment with the α2b splice form. On excision, the patch was superfused with a solution containing 10 mM EGTA to remove endogenous CaM that might adhere to the channel. The current was then recorded continuously (in solutions containing 50 μM free Ca^{2+} and the indicated concentrations of cGMP; or cGMP and CaM) as V_m was switched from -40mV to 40 mV in 1-s intervals. At the beginning, the patch was superfused with 100 μM cGMP to determine saturating currents. In cGMP-free solutions, only small leak currents were measured. During superfusion for roughly 1 min with 3 μM cGMP (a concentration close to the $K_{1/2}$ value), the cGMP-activated current was constant. When the solution was changed to 3 μM cGMP plus 1 μM CaM, the current declined within 30 s to approximately 50% of its previous value. Saturating currents at the beginning and the end of the experiment were identical, and the CaM effect was fully reversible when the patch was superfused for 1 min with 10 mM EGTA (data not shown). Similar results were obtained in six experiments. The CaM effect was similar on the two splice variants, α2a and α2b.

Discussion

Ever since the discovery of the first signaling molecules in olfactory neurons, two rival signaling pathways have been invoked. One hypothesis assumes that all OSNs use cAMP for odorant signaling; the opponent hypothesis states that two independent signaling pathways exist that use either cAMP or IP_3 (29). Another intracellular messenger, cGMP, was considered as an "adaptive" molecule that modulates the cAMP pathway by ill-defined mechanisms (30–32). The report by Juilfs *et al.* (14) and our own results collectively support the notion that some OSNs employ a cGMP pathway for odorant signaling. We show that the cGMP-selective α2 channel is expressed in the same OSNs that express GC-D and PDE2. Furthermore, we and Juilfs *et al.* (14) demonstrate that G_{olf}, ACIII, PDE1C2, and the CNG channel subunits α3 and β1b—characteristic markers for the enzymatic make-up of the prototypical OSNs—are absent from PDE2/GC-D/α2 cells. These findings rule out the coexistence of the known cAMP- and this novel cGMP-signaling pathway. However, we cannot exclude that this subset of OSNs employs other cAMP-signaling components. Indirect support for these conclusions comes from mice with a targeted deletion of the α3 subunit (33). The "necklace" glomeruli in the olfactory bulb are spared from the morphological alterations observed in the typical glomeruli of the null-mice, suggesting that the atypical glomeruli receive innervation from a subset of receptor neurons that use a pathway independent of cAMP signaling.

A precedent for chemosensory signaling using a cGMP-pathway exists in *Caenorhabditis elegans*, where at least 29 different receptor GCs have been identified (34). Several of these receptors have been localized to sensory neurons that also express the CNG channel genes *tax-2* and *tax-4* (35, 36), which produce highly cGMP-selective channels. Thus, it appears that a phylogenetically ancient chemosensory system that is distinct from the system processing volatile odors conveys sensory information by way of a cGMP-, rather than a cAMP-, signaling pathway. Both pathways are endowed with entirely different components and probably evolved independently of each other. It will be a formidable task for future work to unravel the biological function(s) of this unique chemosensory system and to identify the respective physiological ligands.

CNG channels are nonselective cation channels that support inward currents carried by Na^+ and Ca^{2+} ions (for review see ref.

Table 1. Activation parameters of α2 channels

	$V_m = -60$ mV		$V_m = +60$ mV	
	Rat α2a	Rat α2b	Rat α2a	Rat α2b
$K_{1/2}$ (cGMP)/μM (6)	3.7 ± 1.0	4.0 ± 1.4	2.0 ± 0.4	1.7 ± 0.7
n (cGMP) (6)	1.8 ± 0.2	1.7 ± 0.3	2.0 ± 0.3	2.0 ± 0.3
$K_{1/2}$ (cAMP)/μM (6)	441.0 ± 94.0	613.0 ± 83.0	277.0 ± 67.0	396.0 ± 85.0
n (cAMP) (6)	1.6 ± 0.2	1.5 ± 0.2	1.5 ± 0.1	1.5 ± 0.1
I_{cAMP}/I_{cGMP} (12)	0.7 ± 0.1	0.7 ± 0.1	1.0 ± 0.1	1.0 ± 0.1

Mean ± SD of $K_{1/2}$ values and Hill coefficients *n*. The number of experiments is indicated in parentheses.

11). In OSNs that use a cAMP-signaling pathway, the odorant-stimulated rise in $[Ca^{2+}]_i$ (37) plays an important role in both excitation and adaptation. A rise in $[Ca^{2+}]_i$ activates Cl^- channels that carry a large fraction of the odorant-induced receptor current (38–40). Ca^{2+} also stimulates cAMP hydrolysis by the ciliary CaM-dependent PDE1C2 (14, 41), and it attenuates the cAMP sensitivity of the CNG channel by a mechanism involving CaM (28, 42). Both mechanisms terminate the odorant response and lower the sensitivity of the OSN to subsequent stimulation (43). CNG channels containing $\alpha 2$ subunits are roughly as Ca^{2+} permeable as the $\alpha 3\alpha 4\beta 1$b channels (44–47), and stimulation of OSNs equipped with a cGMP-signaling pathway is expected to raise $[Ca^{2+}]_i$.

At present, we can only speculate about a Ca^{2+}-dependent feedback in PDE2/GC-D/$\alpha 2$ cells. The CaM-dependent PDE1C2 is absent from these cells (14), and the CaM action on $\alpha 2$ channels is much weaker than on CNG channels in typical OSNs (42). It is conceivable that adaptation to ligands that control important aspects of behavior differs from the fast and complete adaptation to normal odors in typical OSNs. Alternatively, an unknown Ca^{2+}-binding protein with much higher efficacy than CaM might be the authentic modulator of CNG channels in PDE2/GC-D/$\alpha 2$ cells.

By analogy to what is known in photoreceptors, the shift of the cGMP sensitivity may not be the only action of Ca^{2+} inside PDE2/GC-D/$\alpha 2$ cells. Guanylyl cyclases GC-E and GC-F expressed in retinal photoreceptors are regulated by $[Ca^{2+}]_i$ (48) and not by extracellular ligands. Their Ca^{2+} sensitivity is mediated by a set of guanylyl cyclase-activating proteins (GCAPs), which are members of the large family of Ca^{2+}-binding proteins (for review see ref. 49). GC-D is phylogenetically more akin to the Ca^{2+}-regulated GC-E and GC-F than to receptor GCs-A/B/C, which are activated by peptide ligands. In particular, GC-D and GC-E/F share characteristic sequence similarity in a regulatory domain that is involved in binding of GCAPs (50). This similarity raises the intriguing possibility that GC-D activity is under the dual control of an unknown extracellular ligand and $[Ca^{2+}]_i$.

We thank D. Garbers (Dallas), J. Beavo (Seattle), I. Boekhoff (Stuttgart), and H. G. Körschen (Jülich) for gifts of antibodies, A. Köngeter and W. Bönigk for characterization of antibody CR03B10, and J. Bradley (Paris) for many helpful comments on the manuscript. This work was supported by the European Commission (BIO4-98-0034).

1. Gold, G. H. (1999) *Annu. Rev. Physiol.* **61,** 857–871.
2. Buck, L. & Axel, R. (1991) *Cell* **65,** 175–187.
3. Mombaerts, P. (1999) *Nat. Neurosci.* **2,** 686–687.
4. Bakalyar, H. A. & Reed, R. R. (1990) *Science* **250,** 1403–1406.
5. Jones, D. T. & Reed, R. R. (1989) *Science* **244,** 790–795.
6. Breer, H., Boekhoff, I. & Tareilus, E. (1990) *Nature (London)* **345,** 65–68.
7. Nakamura, T. & Gold, G. H. (1987) *Nature (London)* **325,** 442–444.
8. Frings, S. & Lindemann, B. (1991) *J. Gen. Physiol.* **97,** 1–16.
9. Sautter, A., Zong, X., Hofmann, F. & Biel, M. (1998) *Proc. Natl. Acad. Sci. USA* **95,** 4696–4701.
10. Bönigk, W., Bradley, J., Müller, F., Sesti, F., Boekhoff, I., Ronnett, G. V., Kaupp, U. B. & Frings, S. (1999) *J. Neurosci.* **19,** 5332–5347.
11. Kaupp, U. B. (1995) *Curr. Opinion Neurobiol.* **5,** 434–442.
12. Finn, J. T., Grunwald, M. E. & Yau, K.-W. (1996) *Annu. Rev. Physiol.* **58,** 395–426.
13. Fülle, H.-J., Vassar, R., Foster, D. C., Yang, R.-B., Axel, R. & Garbers, D. L. (1995) *Proc. Natl. Acad. Sci. USA* **92,** 3571–3575.
14. Juilfs, D. M., Fülle, H.-J., Zhao, A. Z., Houslay, M. D., Garbers, D. L. & Beavo, J. A. (1997) *Proc. Natl. Acad. Sci. USA* **94,** 3388–3395.
15. Foster, D. C., Wedel, B. J., Robinson, S. W. & Garbers, D. L. (1999) *Rev. Physiol. Biochem. Pharmacol.* **135,** 1–39.
16. Teicher, M. H., Stewart, W. B., Kauer, J. S. & Shepherd, G. M. (1980) *Brain Res.* **194,** 530–535.
17. Greer, C. A., Stewart, W. B., Teicher, M. H., Kauer, J. S. & Shepherd, G. M. (1982) *J. Neurosci.* **12,** 1744–1759.
18. Misaka, T., Kusakabe, Y., Emori, Y., Gonoi, T., Arai, S. & Abe, K. (1997) *J. Biol. Chem.* **272,** 22623–22629.
19. Baumann, A., Frings, S., Godde, M., Seifert, R. & Kaupp, U. B. (1994) *EMBO J.* **13,** 5040–5050.
20. Bönigk, W., Altenhofen, W., Müller, F., Dose, A., Illing, M., Molday, R. S. & Kaupp, U. B. (1993) *Neuron* **10,** 865–877.
21. Weyand, I., Godde, M., Frings, S., Weiner, J., Müller, F., Altenhofen, W., Hatt, H. & Kaupp, U. B. (1994) *Nature (London)* **368,** 859–863.
22. Yu, W.-P., Grunwald, M. E. & Yau, K.-W. (1996) *FEBS Lett.* **393,** 211–215.
23. Wissinger, B., Müller, F., Weyand, I., Schuffenhauer, S., Thanos, S., Kaupp, U. B. & Zrenner, E. (1997) *Eur. J. Neurosci.* **9,** 2512–2521.
24. Biel, M., Zong, X., Distler, M., Bosse, E., Klugbauer, N., Murakami, M., Flockerzi, V. & Hofmann, F. (1994) *Proc. Natl. Acad. Sci. USA* **91,** 3505–3509.
25. Bönigk, W., Müller, F., Middendorff, R., Weyand, I. & Kaupp, U. B. (1996) *J. Neurosci.* **16,** 7458–7468.
26. Grunwald, M. E., Zhong, H., Lai, J. & Yau, K.-W. (1999) *Proc. Natl. Acad. Sci. USA* **96,** 13444–13449.
27. Gerstner, A., Zong, X., Hofmann, F. & Biel, M. (2000) *J. Neurosci.* **20,** 1324–1332.
28. Liu, M., Chen, T.-Y., Ahamed, B., Li, J. & Yau, K.-W. (1994) *Science* **266,** 1348–1354.
29. Schild, D. & Restrepo, D. (1998) *Physiol. Rev.* **78,** 429–466.
30. Breer, H. & Shepherd, G. M. (1993) *Trends Neurosci.* **16,** 5–9.
31. Kroner, C., Boekhoff, I., Lohmann, S. M., Genieser, H.-G. & Breer, H. (1996) *Eur. J. Biochem.* **236,** 632–637.
32. Zufall, F. & Leinders-Zufall, T. (1998) *Ann. N. Y. Acad. Sci.* **855,** 199–204.
33. Baker, H., Cummings, D. M., Munger, S. D., Margolis, J. W., Franzen, L., Reed, R. R. & Margolis, F. L. (1999) *J. Neurosci.* **19,** 9313–9321.
34. Yu, S., Avery, L., Baude, E. & Garbers, D. L. (1997) *Proc. Natl. Acad. Sci. USA* **94,** 3384–3387.
35. Coburn, C. M. & Bargmann, C. I. (1996) *Neuron* **17,** 695–706.
36. Komatsu, H., Mori, I., Rhee, J.-S., Akaike, N. & Ohshima, Y. (1996) *Neuron* **17,** 707–718.
37. Leinders-Zufall, T., Greer, C. A., Shepherd, G. M. & Zufall, F. (1998) *J. Neurosci.* **18,** 5630–5639.
38. Kleene, S. J. (1993) *Neuron* **11,** 123–132.
39. Kurahashi, T. & Yau, K.-W. (1993) *Nature (London)* **363,** 71–74.
40. Lowe, G. & Gold, G. H. (1993) *Nature (London)* **366,** 283–286.
41. Yan, C., Zhao, A. Z., Bentley, J. K. & Beavo, J. A. (1996) *J. Biol. Chem.* **271,** 25699–25706.
42. Chen, T.-Y. & Yau, K.-W. (1994) *Nature (London)* **368,** 545–548.
43. Kurahashi, T. & Menini, A. (1997) *Nature (London)* **385,** 725–729.
44. Perry, R. J. & McNaughton, P. A. (1991) *J. Physiol.* **434,** 70P.
45. Frings, S., Seifert, R., Godde, M. & Kaupp, U. B. (1995) *Neuron* **15,** 169–179.
46. Picones, A. & Korenbrot, J. I. (1995) *Biophys. J.* **69,** 120–127.
47. Dzeja, C., Hagen, V., Kaupp, U. B. & Frings, S. (1999) *EMBO J.* **18,**
48. Koch, K.-W. & Stryer, L. (1988) *Nature (London)* **334,** 64–66.
49. Polans, A., Baehr, W. & Palczewski, K. (1996) *Trends Neurosci.* **19,** 547–554.
50. Lange, C., Duda, T., Beyermann, M., Sharma, R. K. & Koch, K.-W. (1999) *FEBS Lett.* **460,** 27–31.
51. Rhoads, A. R. & Friedberg, F. (1997) *FASEB J.* **11,** 331–340.